Photometric calibration of an in situ broadband optical thickness monitoring of thin films in a large vacuum chamber

David Hofman, Benoit Sassolas, Christophe Michel, Laurent Balzarini, Laurent Pinard, Julien Teillon, Bernard Lagrange, Eleonore Barthelemy-Mazot, Gianpietro Cagnoli

applied optics

Photometric calibration of an *in situ* broadband optical thickness monitoring of thin films in a large vacuum chamber

David Hofman,[1,*] Benoit Sassolas,[1] Christophe Michel,[1] Laurent Balzarini,[1] Laurent Pinard,[1] Julien Teillon,[1] Bertrand David,[1] Bernard Lagrange,[1] Eleonore Barthelemy-Mazot,[1] and Gianpietro Cagnoli[1,2]

[1]Laboratoire des Matériaux Avancés (LMA), IN2P3/CNRS, F-69622 Villeurbanne, France
[2]Université Claude Bernard Lyon 1 (UCBL), 69622 Villeurbanne Cedex, France
*Corresponding author: d.hofman@lma.in2p3.fr

Received 14 October 2016; revised 5 December 2016; accepted 13 December 2016; posted 14 December 2016 (Doc. ID 278693); published 11 January 2017

To improve the *in situ* monitoring of thin films at the Laboratoire des Matériaux Avancés, a broadband optical monitoring of the coated thin films was developed and installed in the biggest ion-beam sputtering machine in the world. Due to the configuration of the coating machine and the chamber strain under vacuum, a standard calibration procedure is impossible and a double-beam optical system is not suitable. A novel theoretical and practical solution to calibrate the measurements was found and is described in this paper. Some relevant results achieved thanks to this technique are discussed as well.

OCIS codes: (310.1860) Deposition and fabrication; (120.5700) Reflection; (120.5240) Photometry.

https://doi.org/10.1364/AO.56.000409

1. INTRODUCTION

The Laboratoire des Matériaux Avancés (LMA) has installed a full automated broadband optical monitoring [1–5] in its large ion-beam sputtering (IBS) machine (Fig. 1). This machine, designed for the deposition of the optics of the gravitational wave detector Virgo [6] (and also the optics of Advanced Ligo [7]), is unique for its custom-developed design: a vacuum chamber of 2.2 m × 2.2 m × 2 m that can accept optics up to 1 m in diameter.

The motivations that lie behind the installation of this optical system are multiple, but two of them are crucial for the next few years. For the next generations of the gravitational interferometers (Virgo, Ligo, Kagra, etc.), the coatings needed on the optics are increasingly demanding in terms of optical performance. This performance goes through a precise monitoring of what is deposited on the optic. For example, the antireflection (AR) coatings that will be needed on the optics of these experiments will be as low as 50 ppm (0.005%) of reflection at the laser wavelength. This cannot be achieved with good repeatability using the quartz crystal microbalance monitoring that was used until now in the coater. The laboratory never reached good repeatability with the quartz microbalance, succeeding less than 10% of the coating runs with a twice higher success criterion ($R < 100$ ppm at 1064 nm). Simulations of coating runs monitored by quartz crystal microbalance were done (5000 of them) to calculate the production yield of a four-layer AR coating (the one that will be the guideline in this paper). Random errors generated by a uniform law of 1% (which is the best precision of the quartz monitoring that one can achieve) and 2% of layer thicknesses were applied to the four layers of the design used (no link between the layers), and the success criterion of R being inferior or at least equal to 100 ppm (0.01%) at 1064 nm was applied. As shown in Fig. 2, we can see that even small random errors of thicknesses can destroy the optical performance of the deposited stack. The bigger the errors are, the wider is the possibility of the result of reflection at 1064 nm. The calculated yields for 1% and 2% random errors are 40% and 22.5% of the runs, respectively. These low yields explain why this design was never coated repeatedly with success using quartz monitoring.

For various reasons, the coatings deposited on the optics (the mirrors, for example) that constitute the arm cavities of the interferometers need to be paired. They need to have the same thickness uniformity (which is not the scope of this paper), and they need to have the same coatings, in term of layer thicknesses, that are deposited on them so they have the same optical properties. The coater now has the ability to coat two large optics at the same time in planetary motion of the substrates, but in the future, the optics will be increasingly larger so that only one substrate will be coated at the same

Fig. 1. Photograph of the IBS machine in the back of the clean room. Credits: Cyril FRESILLON/LMA/CNRS Photothèque.

time. For this reason, an optical monitoring will allow the pairing of multiple optics between several coating runs by maintaining the same layer thicknesses.

When this machine was designed 20 years ago, no optical monitoring was expected to be installed in it. No viewport was usable to directly point a light beam on the substrate surface. For this reason, the entire optical system (but not the spectrometer) was installed inside the machine (Fig. 3). Another restriction on the monitoring operation is that only measurements in reflection can be done. Because of the massive door in stainless steel and the complex rotating mechanics that activate the substrate rotation, no hole could be placed behind the substrate to allow transmission measurements.

The deformations of the chamber due to the vacuum alter the position of the substrates because the holder is mounted on the loading door. Measurements in reflection are much more sensitive to changes of the surface position than the measurements made in transmission. That is why a calibration of the optical system before the coating run can be tricky. There are also some inherent effects in a long coating run, discussed further in this paper, that makes useless the use of a reference beam (typically, a double-beam setup of the optical system, as in some spectrometers).

This paper will first rapidly present the optical setup inside the coating machine and the mechanical issues in Section 2. Then, the heart of the subject will be addressed in Section 3: the calibration of the optical system. Some results of depositions monitored by the calibrated system will be briefly presented in Section 4, and a conclusion will be given in the last section.

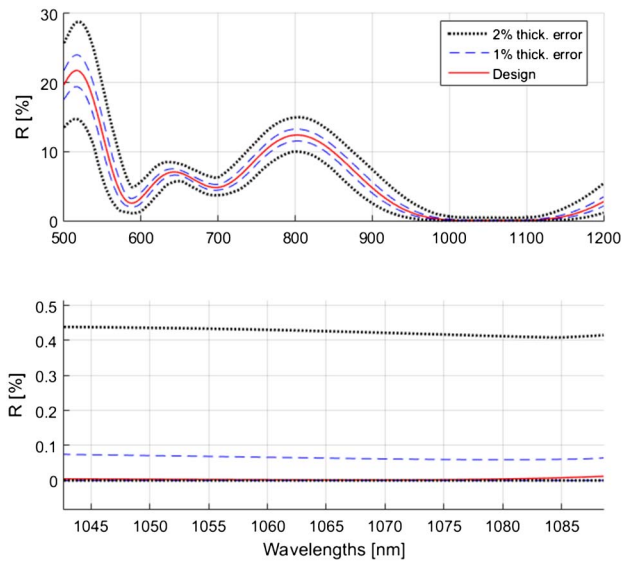

Fig. 2. Graphs of the simulated coating of the four-layer AR monitored by quartz crystal microbalance. The errors of thicknesses are 1% for the blue envelopes and 2% for the black ones. The plain curve in red is the nominal design of the four-layer AR at 1064 nm. The second graph at the bottom is a zoom of the first graph in the region around 1064 nm.

2. SETUP

An optical system was designed and installed inside the coater, allowing the *in situ* monitoring of the thin-film growth. A double telescope that focuses a 8 mm diameter spot at almost 1 m from the deposition plane (i.e., the first surface of the substrate), allows the measurement by reflection of the thin films that are being deposited in the machine (Fig. 3).

The light falls in the middle of the holder rotation so that not only a big substrate, but also a batch of little optics, through the intermediary of a witness sample situated in the middle of the substrate holder, can be monitored.

The optical system uses a MCS 600 modular spectrometer from Zeiss Company on a broadband spectrum of monitoring wavelengths (from 500 to 1016 nm) via two silica fibers (one for emission, another for reception). These fibers cross the machine wall without couplers to maximize the light flux that enters the optical system. The designed optical system ensures that no parasite light (plasma of ion source, IR lamp, etc.) is read by the spectrometer, leading to errors in the monitoring, and also ensures that almost no sputtered matter can go on the optics during the deposition runs.

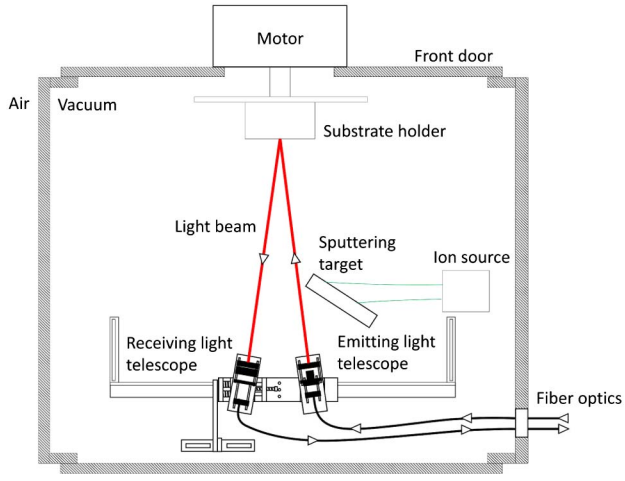

Fig. 3. Diagram of the optical system setup inside the coating machine seen from above. The distance of the substrate from the telescopes is about 1 m.

A halogen light, optimally coupled into the emission fiber, ensures that minimal integration times on the spectrometer can be achieved (12 ms), making it possible to acquire spectra in a short time. The light emitted falls on the substrate with an angle of incidence of 10°. The surface of the substrate (as well as the rear surface) reflects the light toward the second telescope, coupling it into another optical fiber connected to the spectrometer.

Looking at Fig. 3, one can quickly see that if the surface of the measured substrate is changing its position (tilt and perpendicularly to the deposition plane), the path of the reflected light will be modified, and the coupling into the fiber will be different. Unfortunately, this is the case in this setup when the machine is pumping down and the atmospheric pressure is pressing the door against the seal and the walls.

3. CALIBRATION

Usually, when one wants to make an absolute measurement (in transmission or reflection) of an optical sample, three measurements need to be done (in a single-beam optical assembly): the reference, the dark, and the sample measurement. The reference is the raw spectrum of the total flux delivered by the light source, passing through all the optics, without the sample to measure. In the case of a reflection measurement, a reference mirror with a known optical response is used. The dark is the raw spectrum measured when the light source is cut off (the plasma light inside the IBS chamber is not coupling into the fiber). In this case, the noise of the detector and the parasite light from outside the experience are taken into account. Finally, the sample measurement is taken when the optical piece of interest is on the light path and the corresponding raw spectrum is recorded. Let these be measured raw spectra R, D and S, respectively.

So, the normalized transmission or reflection of a sample, with respect to the total flux of light delivered by the source is (in percentage)

$$\text{Transmission|Reflection} = \frac{S - D}{R - D} \cdot 100. \quad (1)$$

Before using the optical monitoring, we need to do the reference inside the coating machine on a mirror (protected silver in our case) with the optical system. The dark can be done easily at any moment with a motorized shutter in front of the light source.

Due to the large size of the coating chamber, the pumping process takes several hours. So, for convenience, the reference is done at the atmospheric pressure and then the witness substrate is mounted at the reference position for monitoring. Some measurements of the raw spectrum of a bare substrate (fused silica) at atmospheric pressure and under vacuum were done (Fig. 4).

The signal has changed during pumping (up to 20% between the two curves), showing a change in the light path inside the machine. We do not know for sure the way the chamber is distorted under vacuum conditions. It is clear that the door is pressing against the seal, thus advancing the deposition plane (first surface of the substrate). So, we cannot adjust the optical settings under vacuum to compensate the beam displacement;

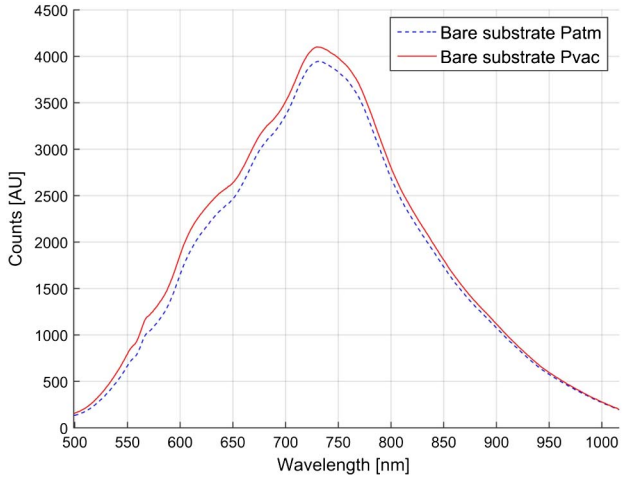

Fig. 4. Graphics of the raw spectrum measured on a bare substrate (fused silica) at atmospheric pressure (blue dotted line) and under vacuum (red line).

we only have the raw spectra that we can measure at different times of the deposition process to help. These two lines are repeatedly measured at the same values (Fig. 4), removing the substrate and putting it back on the holder between different tests, provided that the door is closed in the same way between the measurements at atmospheric pressure.

Due to this, one can immediately say that if we do the ratio between the two spectra of the Fig. 4 and multiply it by the measurements done during deposition, the problem will be solved. But this would introduce another problem during measurement. Until now, we only looked at the light beam reflected by the first surface of the substrate.

In reflection measurement, the light flux coming from the rear surface must be taken into account (Fig. 5). Assuming that we apply a simple coefficient to the measurements, it would be equivalent to say that during the whole coating run, the flux coming from the first and the second surface will behave in the same fashion. This is wrong, because the flux from the rear face is coupled differently into the fiber from the one coming from the first surface. A correction for each surface needs to be done.

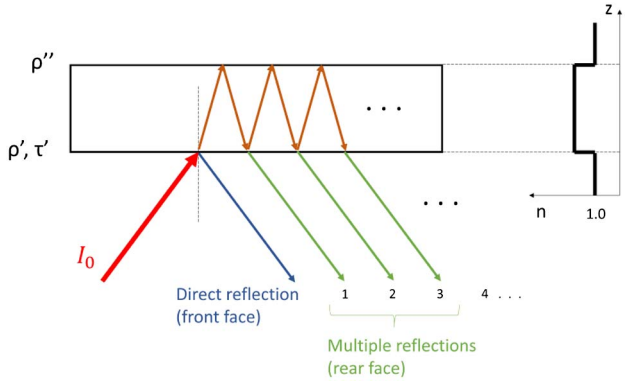

Fig. 5. Diagram of the multiple internal reflections of an incident light beam on a bare substrate. The transmitted light is not of interest and therefore not shown here. n is the refractive index of the substrate.

Let ρ' and τ' be the reflection and the transmission coefficients of the first surface of monitored substrate, and let ρ'' be the reflection coefficient of the second surface (Fig. 5). I_0 will be the incident flux of light, and finally, S_0 the signal measured of all the beams reflected. For the sake of clarity, from now on we will suppose that these quantities are wavelength dependent (moreover, they are measured at monitored wavelengths). Having these quantities, we can write

$$S_0 = \rho' I_0 + I_0 \tau'^2 \rho'' + I_0 \tau'^2 \rho''^2 \rho' + \ldots, \tag{2}$$

where the dots at the end are the infinite sum of the internally reflected beam between the first and the second surface of the substrate. There is another implicit hypothesis when 2 is written. We assume that beams 1, 2, 3, 4, …. (Fig. 5) enter into the fiber with the same efficiency. This equation can be rewritten as an explicit sum

$$S_0 = \rho' I_0 + I_0 \rho''(1-\rho')^2 \cdot \frac{1}{1-\rho'\rho''}, \tag{3}$$

where τ' has been replaced by $1-\rho'$, assuming the coating and the substrate have negligible absorption.

Now, if we use this Eq. (3) to express the signal S_c measured on the same substrate but under vacuum conditions we can write

$$S_c = \alpha' \rho' I_0 + \alpha'' I_0 \rho''(1-\rho')^2 \cdot \frac{1}{1-\rho'\rho''}, \tag{4}$$

where α' and α'' are the correction coefficients of the flux coming, respectively, from the first surface and the second surface of the substrate.

What is important to know here is that what is measured at P_{atm} is no longer valid under vacuum due to the deformations on the substrate holder. Also, the mathematical form of Eq. (4) applies a single correction coefficient to all the back-reflected light because we treat the multiple reflections as one unique beam.

Now the heart of the game is to find these two correction coefficients α' and α''.

A. Measurement of α'

To find the coefficient α', we simply measure the bare substrate with coefficient α'' null. This can be easily done by taking a substrate of the same type as the one used for the coating monitoring and grinding the back surface (Fig. 6). The light transmitted by the first surface is integrally diffused, and a negligible light comes back from the rear. From the double measurement in atmospheric pressure (P_{atm}) S_0^* and in vacuum (P_{vac}) S_c^*, we can find α' as shown below

Fig. 6. Bare substrate (fused silica) with one grounded side. Left, the clean side; right, the ground surface.

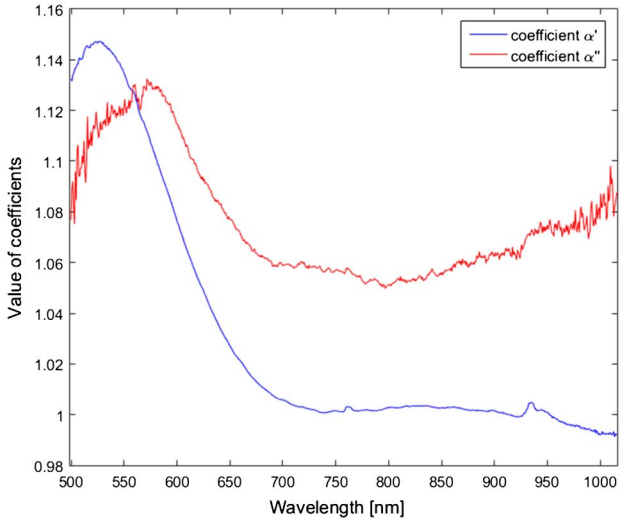

Fig. 7. Graph of the coefficient α' and α'' calculated on the monitoring wavelengths of the optical system.

$$\left.\begin{aligned} S_0^* &= \rho' I_0 \\ S_c^* &= \alpha' \rho' I_0 \end{aligned}\right\} \qquad \alpha' = \frac{S_c^*}{S_0^*}. \tag{5}$$

As seen in Fig. 7, the coefficient α' is a significant correction of the flux.

B. Measurement of α''

Finding α'' is little more complicated, because in general we cannot separate the second reflection from the first.

In the cycle of the deposition process, we do the reference measurement so we have the quantity I_0, which is the ratio between the raw spectrum acquired from the reference mirror and the normalized reflection of the mirror (given by the manufacturer by measurement with another reference mirror). So, I_0 is the total flux of light measured. Then, the mirror is replaced by the witness sample, and two measurements are done: the first one at P_{atm} [Eq. (3)], the second one at P_{vac} [Eq. (4)], when the coating chamber is under vacuum ready to coat the substrate. By doing so, we have, respectively, the two raw spectra S_0 [Eq. (3)] and S_c.

To calculate α'', we have to make an assumption that takes place just before the coating run begins, when nothing has been deposited on the substrate

$$\rho' = \rho'' = \rho_b, \tag{6}$$

where ρ_b stands for "bare" substrate. To be accurate, we use a fused silica substrate where the two faces are free of coating, so the previous assumption is true. According to this statement, S_c becomes

$$S_c = I_0 \cdot \rho_b \left[\alpha' + \alpha'' \cdot \frac{1-\rho_b}{1+\rho_b}\right]. \tag{7}$$

This gives us directly the coefficient α'' (Fig. 7)

$$\alpha'' = \left[\frac{S_c}{I_0 \cdot \rho_b} - \alpha'\right] \cdot \frac{1+\rho_b}{1-\rho_b}. \tag{8}$$

Now we need to determine ρ_b; from Eqs. (3) and (6) we can write

$$S_0 = \rho_b \cdot I_0 + I_0 \cdot \rho_b \cdot (1-\rho_b)^2 \cdot \frac{1}{1-\rho_b^2}. \quad (9)$$

So, ρ_b comes immediately

$$\rho_b = \frac{S_0}{2 \cdot I_0 - S_0}. \quad (10)$$

Now, we have ρ_b, so we can express α'' with the measurements done before the beginning of the deposition

$$\alpha'' = \frac{S_c}{S_0}\frac{2I_0 - S_0}{I_0 - S_0} - \frac{\alpha' \cdot I_0}{I_0 - S_0}. \quad (11)$$

If we define S as the raw spectrum of the coated substrate measured during deposition [from Eq. (4)]

$$S = \frac{\alpha'\rho'(1-\rho'\rho_b)I_0 + \alpha''(1-\rho')^2\rho_b I_0}{1-\rho'\rho_b}, \quad (12)$$

with $\rho'' = \rho_b$ (no deposition on the back surface), then, knowing α' and α'' from Eq. (4), we work out ρ' during deposition. Where ρ' is defined by the equation

$$\rho' = \frac{2\alpha''\rho_b - \alpha' - R\rho_b + \sqrt{\Delta}}{2\rho_b(\alpha'' - \alpha')}, \quad (13)$$

with $R = \frac{S}{I_0}$ and Δ given by

$$\Delta = (\alpha' - \rho_b R)^2 + 4\alpha''\rho_b(\alpha' - R)(\rho_b - 1). \quad (14)$$

Finally, we can replace ρ' in Eq. (3)

$$S_0 = \rho' I_0 + I_0\rho_b(1-\rho')^2 \cdot \frac{1}{1-\rho'\rho_b}. \quad (15)$$

We get the corrected raw spectrum of the witness substrate as if it were measured in atmospheric conditions. To finish, we calculate the reflection R, the reflection of the substrate first surface

$$R_0 = \frac{S_0}{I_0}. \quad (16)$$

So finally, we have the corrected front reflection of the coated substrate.

C. Signal Drift

However, even with the help of this calibration procedure, there is still another effect that must be taken into account: the signal drift during time. Of course, we are talking about the flux drift of light source used for the spectrophotometric measurements, but not only. Inside the machine, with the optical setup and under vacuum conditions, we measured the signal drift during several hours (equal to the deposition time of some coatings). The results of these measurements are shown in Fig. 8.

The measurements were made by acquiring a raw spectrum of a mirror every 5 min under vacuum conditions (beginning when the chamber was at working pressure, 10^{-4} mbars), without the plasma source on (anyway, the light of the plasma source is not coupled into the optical system and is not measurable). This was done for almost 12 h inside the machine. Then, we took the first acquisition as the reference for the whole series, and we calculated the relative difference with the other measurements

$$D = \frac{M_n - M_1}{M_1} \cdot 100, \quad (17)$$

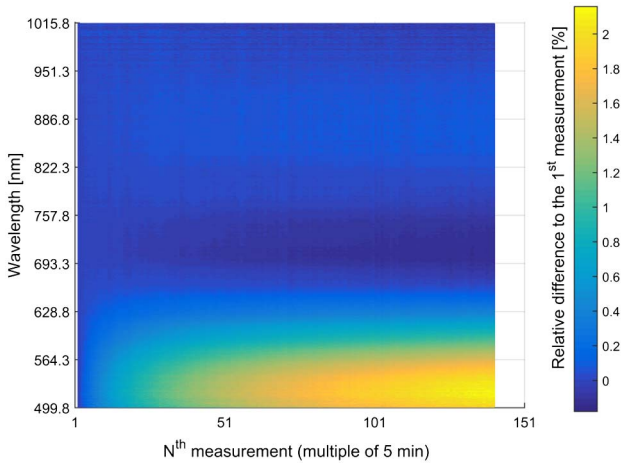

Fig. 8. 3D plot of the signal drift during time, measured inside the coating machine with the optical monitoring. The total length of the measurement is about 12 h.

where D is the relative difference in percentage, M_n is the nth acquisition, and M_1 is the first acquisition.

The variation is strongly chromatic, and the amplitude after several hours reaches almost 2.5% around 550/600 nm. This last observation was incompatible with the lamp manufacturer claim: the lamp is voltage controlled; thus, the drift should be negligible. So, the spectrometer was moved and used with a simple optical setup outside the machine, at atmospheric conditions, to see if the results were the same. The drift of the lamp can be seen in Fig. 9.

The comparison between the two Figs. 8 and 9 is straightforward: the flux drift outside the machine does not match at all the one measured *in situ*. The lamp alone has a drift of only of 0.3% at maximum during almost 12 h, while the drift measured *in situ* is almost a factor of 10 higher with an opposite sign. We can note that the drift seen in Fig. 9 is contained in the drift measured *in situ* (Fig. 8), because the lamp itself is

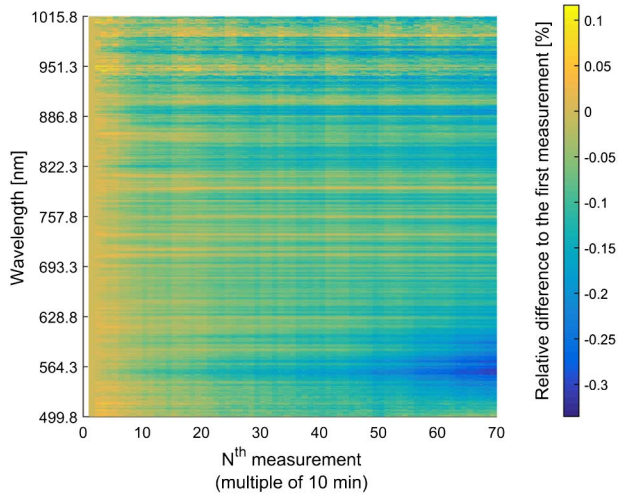

Fig. 9. 3D plot of the lamp flux drift during time measured outside the coating machine. Be aware that the color scale is different from the one in Fig. 8.

drifting in flux during deposition and the *in situ* drift measurement.

The sign of the flux change *in situ* (increasing for some wavelengths) during the time, the amplitude of the drift, and the strong chromaticism of the drift, made us think that another phenomenon than the one associated with the lamp is at work here. We are not sure about what is happening inside the machine—maybe the chamber has a very long time of distortion before being at a mechanical steady-state or the substrate holder is moving a little during the whole coating run due to thermal and mechanical distortions. But looking at Fig. 8, we are sure that the light path has changed again. So, a correction of the calibration is needed. This correction has to be along the whole coating run and begins just when the first layer is about to be deposited. Another thing to know is that if the optical system is moved or adjusted, this drift measurement has to be mapped again, because in our setup, the light will not be coupled in the same manner, thus changing the flux drift along all the monitored wavelengths.

The coefficient α' takes care of the first distortion of the chamber when the vacuum is made and the door sealed by the atmospheric pressure, between the measurement of the witness substrate at air and when the deposition of the first layer is ready to begin. Then, this coefficient remains constant and is integrated in the whole calibration calculus, which seems incompatible with the drift seen inside the chamber. So, α' needs to be corrected by the drift acquired

$$\alpha'_c(t) = \alpha'(t_0) + d^m(t) \cdot \alpha'(t_0), \tag{18}$$

where $\alpha'_c(t)$ is the drift corrected coefficient at time t, $\alpha'(t_0)$ is the coefficient calculated at the beginning of the deposition, and $d^m(t)$ is the normalized drift measured during the drift test (Fig. 8).

This correction is self-consistent: the coefficient α' is corrected from the drift, and this coefficient is used for the rest of the calibration so no other part of the calculus needs to be corrected; α'' is automatically corrected too, because it contains α'.

D. Validity Domains of the Calibration

Let us get back to a point we passed over quickly at the beginning of the previous section. We made the assumption that the reflection of the front surface of the witness substrate is equal to the reflection of the rear surface [Eq. (6)]. This is only true if we collect all the light coming from the rear surface into the optic fiber, or if there is no coating on the rear surface that would change its reflection properties.

Another situation occurs when the substrate is thick enough so the backside reflection is not coupled in the optical system (or has a wedge such as the beam is deviated enough). So, the problem is equal to a light beam falling on a semi-infinite substrate, with just the front surface that reflects the light. In this case, the calibration is simple: the coefficient α'' and the reflection coefficient ρ'' are equal to zero. The calibration is just the ratio α' (still drift-corrected) that multiplies the substrate measurement during the coating process.

By the way, a direct solution to simplify the calibration would be, in this case of an optical monitoring system operating exclusively in reflection, to systematically grind the rear face of the witness substrate in order to eliminate the rear reflection. But in many cases, the witness sample is desired for several optical characterizations (in transmission most of the time) or, as much as we can, we want to monitor the "real" optic, so we cannot grind it.

This resolves the two cases where no or all the light from the rear surface is collected. But there is a trickier case, where the substrate has no wedge and has a thickness such that not all the light from the rear surface is collected. In this case, we cannot make the assumption of Eq. (6) anymore. We have to know what part of the light is coupled into the optical system in reception.

So, in our case with the optical setup shown in Fig. 2, we modeled it under the ZEMAX optical simulation software, and we calculated the coupling efficiency of the beam coming from the rear surface inside the reception fiber with respect to the substrate thickness (fused silica). The result of this calculation can be seen in Fig. 10.

Three zones can be seen on this graph:

- The first zone, on the left, from 0 to 6.5 mm of substrate thickness, corresponds with a coupling efficiency (all wavelengths summed) from 1 to 0.995. This zone is where all the flux of light coming from the rear surface is acquired.
- The second zone, in the middle, from 6.5 to 28 mm of substrate thickness, corresponds with a coupling efficiency (all wavelengths summed) from 0.995 to 0.0055. This zone is where a fraction of the light coming from the rear surface is acquired.
- The last zone, on the right, from 28 mm of substrate thickness, corresponds with a coupling efficiency (all wavelengths summed) from 0.0055 to 0. This zone is where no light coming from the rear surface is acquired.

To sum up the different cases, if we take the reflections of the two surfaces as we defined them, we have for the first zone

$$\rho' = \rho'' = \rho_b. \tag{19}$$

For the second zone we have

$$\rho' = A \cdot \rho'' = \rho_b, \tag{20}$$

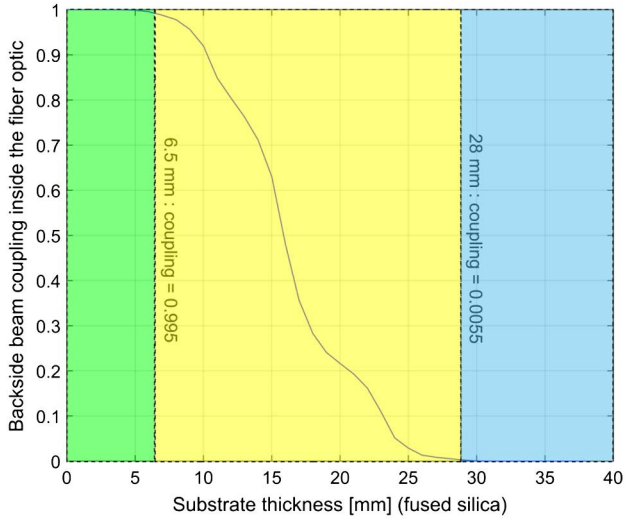

Fig. 10. Coupling efficiency of the reflected beam from the rear of the witness substrate with respect to its thickness.

where A is the ratio of flux coming from the front and the rear face of the substrate. And for the last zone we have

$$\rho' = \rho_b, \tag{21}$$

$$\rho'' = \alpha'' = 0. \tag{22}$$

The delimitation of the three zones is arbitrary and corresponds with a loss (or a gain) of 0.5% of the flux coming from the rear surface. This arbitrary criterion is less than the total loss of the optical system and can be neglected in our setup. The calculation of the coefficient A needs the knowledge of the flux lost with the thickness of the witness (or the real) substrate in the frame of the optical setup installed.

There is a last case where the backside reflection is entirely or partially collected and/or the rear face of the substrate has a coating on it. So, the reflectivity of the first surface does not match the reflection of the back surface. Then, zone 1 and zone 2 become a unique zone, where the coefficient A has to be used, because Eq. (19) is no longer valid. In this case, A needs to be known at all the wavelengths monitored. Moreover, A depends now on two quantities: the ratio of the surface reflections between the two sides of the substrate (due to the coating already present on one of two surfaces) and the fraction of backside-reflected light (ideally at every wavelength monitored).

4. RESULTS

Here we present the results of a series of coating runs monitored by the optical system presented and calibrated as described previously. There is a total of six coatings of a four-layer AR stack that were successively deposited and characterized. The success criterion of these coatings was a reflection lower than 100 ppm (0.01%) at 1064 nm.

The broadband optical monitoring was using a discrepancy function between the measured spectrum (calibrated) at given time t and the theoretical spectrum at the end of the current layer

$$\chi_i(t) = \sqrt{\frac{1}{L}\sum_{j=1}^{L}[R_{\text{th}}(\lambda_j)\cdot 100 - R_{m\cdot}(\lambda_j, t)\cdot 100]^2}, \tag{23}$$

where $\chi_i(t)$ is the discrepancy function at layer i and at given time t, L is the number of wavelengths monitored, λ_j is the jth wavelength monitored, R_{th} and $R_{m\cdot}$ are, respectively, the theoretical and the measured reflection spectrum (calibrated) at given time t. Figure 11 shows the *in situ* measured spectra at the end of each layer compared to the theoretical spectrum. We can see that the calibration procedure gives good results on the shape of the measured spectra: the measured spectra are very close to the theoretical ones. The discrepancies that can be seen in this figure between the theoretical curve and the measured one are mainly due to the overshooting of matter at each layer of the stack. The algorithm used to determine the time to stop the coating does not yet take into account the time needed to close the shutter. We estimate that the overshooting is between 1 and 2 nm per layer. But let us be more quantitative and look at the value of the discrepancy function at the end of each layer.

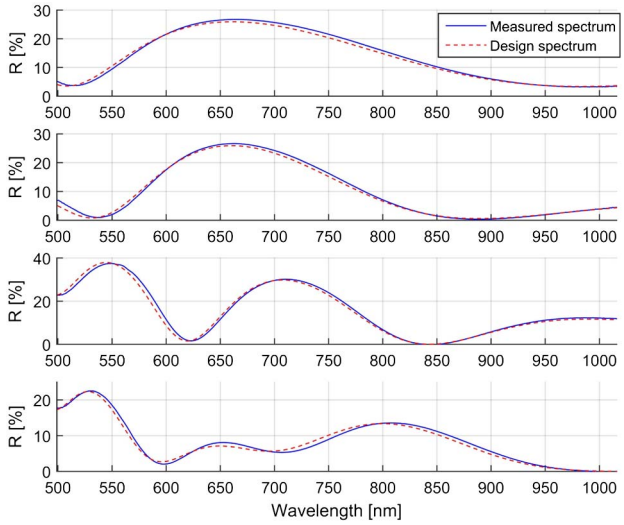

Fig. 11. Graphs of the final measurements *in situ* done by the optical monitoring (blue lines) at the end of each layer of a four-layer AR stack (Run 2). The red line is the theoretical spectrum of the stack at the end of the current layer.

In Fig. 12, the values of the discrepancy function [Eq. (23)] at the end of each layer for the four coating runs are displayed; their precise values can be found in Table 1.

It can be seen that the values are relatively small for the Runs 1 to 4, thus indicating a good stopping ability of the monitoring system. Another thing to see is that from one run to another, the values are nearly the same, indicating that the optical monitoring has good repeatability. All the coating tests succeeded with the criterion of success: the measured reflectivity at 1064 nm were: 12, 46, 28, and 20 ppm.

For the two last Runs (5 and 6) the χ_i are higher than the ones for the first runs. This is because the monitored substrates were large (250 mm diameter and 100 mm thickness). Due to the mechanical configuration of the substrate holder, the

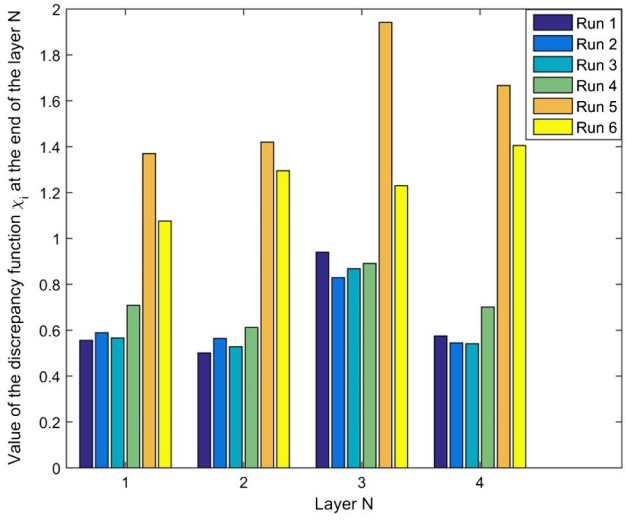

Fig. 12. Bar graph of the discrepancy function values at each end of the four layers deposited in the six coating runs.

Table 1. Final Values of the Discrepancy Function Measured at the End of Each Layer of Each Coating Run with the Final Reflection Value *R* at 1064 nm[a]

	L1	L2	L3	L4	*R* [ppm]	*D* [mm]	*T* [mm]
Run 1	0.556	0.501	0.94	0.575	12	25.4	6
Run 2	0.589	0.564	0.829	0.545	46	25.4	6
Run 3	0.566	0.528	0.868	0.541	28	25.4	6
Run 4	0.709	0.612	0.891	0.701	20	25.4	6
Run 5	1.370	1.420	1.942	1.667	14	250	100
Run 6	1.076	1.295	1.230	1.405	82	250	100

[a]LN is the Nth layer, D is the diameter of the substrate monitored, and T is the thickness.

calibration measurements of the reference and the substrate at air were done in completely different optical mounts. So, it is possible that there were some differences between their first surface positions, so that the two light paths do not match exactly for the two measurements, leading to some errors in calibration.

For such a thick substrate, where the light coming from the rear surface is not coupled, there is an alternative to the reference measurement on the mirror that we did not have the time to test and use, but that we will briefly discuss here.

Instead of measuring the reference (on the mirror) just by closing the door, there is the possibility of skipping this step of the calibration and doing it directly on the substrate to coat inside the machine when a vacuum is made. Based on the well-known reflectivity of the substrate, we can deduce the total flux of the lamp gathered after the multiple deformations of the machine during pumping by this simple relation

$$I_0 = \frac{S}{r_S}, \tag{24}$$

where I_0 is the total flux delivered and gathered, S is the raw spectrum of the substrate measured under vacuum just before the coating run, and r_S is the theoretical reflection of one face of the substrate.

Obviously, using such a substrate (fused silica) to make the reference measurement would induce a faint signal gathered into the optical system. Raising the integration time of the spectrometer and making multiple measurements will increase the signal to noise (S/N) ratio to provide a clean spectrum for the calculation of I_0. Also, in this case, the substrate is thick enough to reduce the whole calibration to the simple coefficient α'.

However, the optical monitoring succeeded in compensating the error and achieving the following reflections at 1064 nm: 14 ppm (Run 5) and 82 ppm (Run 6).

5. CONCLUSION

In this paper, we described the optical setup used in reflection for the broadband monitoring of thin-films growth inside the biggest IBS coating machine in the world. We also presented a calibration procedure that ensures the accuracy of measurements, despite the severe conditions for reflection acquisition. We showed that the calculations can provide the change in optical characteristics of the first surface only, forgetting the rear face of the substrate. We also showed the domains of validity for this technique of signal processing, adapting the calculation for various types of substrates to measure.

Finally, we gave some examples of successful coating runs monitored by the optical system and calibrated with the solution presented in this paper, proving its accuracy and repeatability.

Funding. LABEX Lyon Institute of Origins (ANR-10-LABX-0066); Université de Lyon (ANR-11-IDEX-0007).

REFERENCES

1. B. Vidal, A. Fornier, and E. Pelletier, "Optical monitoring of nonquarter-wave multilayer filters," Appl. Opt. **17**, 1038–1047 (1978).
2. L. Li and Y. H. Yen, "Wideband monitoring and measuring system for optical coatings," Appl. Opt. **28**, 2889–2894 (1989).
3. D. Ristau, H. Ehlers, T. Gross, and M. Lappschies, "Optical broadband monitoring of conventional and ion processes," Appl. Opt. **45**, 1495–1501 (2006).
4. B. Badoil, "Controle spectrophotometrique large bande de filtres interferentiels en cours de depot," Ph.D. dissertation (Universite Paul Cezanne Aix Marseille III, 2007).
5. H. Ehlers, S. Schlichting, C. Schmitz, and D. Ristau, "Adaptive manufacturing of high-precision optics based on virtual deposition and hybrid process control techniques," Chin. Opt. Lett. **8**, 62–66 (2010).
6. The Virgo Collaboration, "Advanced Virgo: a second-generation interferometric gravitational wave detector," Classical and Quantum Gravity **32**, 024001 (2015).
7. The LIGO Scientific Collaboration, "LIGO: the Laser Interferometer Gravitational-Wave Observatory," Rep. Prog. Phys. **72**, 076901 (2009).